

A uniformly moving and rotating polarizable particle in thermal radiation field: frictional force and torque, radiation and heating

G. V. Dedkov and A.A. Kyasov

Nanoscale Physics Group, Kabardino-Balkarian State University, Nalchik, 360000, Russia

Abstract—We study the fluctuation-electromagnetic interaction and dynamics of a small polarizable particle with own rotation and relativistic velocity moving in a vacuum background of arbitrary temperature. A full set of equations describing decelerating tangential force, frictional torque (at arbitrary direction of angular velocity) and intensity of nonthermal and thermal radiation is obtained, along with equations describing the particle dynamics and kinetics of heating. An interplay between different parameters is discussed. Numerical calculations are given in the case of graphite particles.

1. Introduction

Quantum zero-point fluctuations of the electromagnetic field in vacuum cause the Casimir attraction between neutral conducting bodies [1]. When the bodies are moving, they may pull off real photons from the fluctuating QED vacuum [2]. In this relation, it is worthwhile to mention a phenomenon of Zel'dovich' superradiance [3], when a rotating cylinder amplifies certain waves of incident electromagnetic radiation. Moreover, in dynamically and thermally nonequilibrium configurations related with objects in relative motion, the interacting bodies experience not only the action of attractive/repulsive forces and heating/cooling effects, but also frictional forces and mechanical torques [4-17] (one should note that the reference list is not complete). Despite its minuteness, the exchange of momentum by light-matter interaction is responsible for various phenomena ranging from the formation of cometary tails and thermal radiation of cosmic dust to the trapping and cooling of nanoparticles down to single atoms.

However, unlike the longstanding issues related to the fluctuation-electromagnetic forces and heat exchange, much less attention has been paid to thermal and nonthermal radiation effects produced by moving/rotating polarizable nanoparticles [14–17]. Thus, in [14,15] the radiation produced by a particle rotating in vacuum was studied, whereas in [16,17] the impact of uniform relativistic motion on the spectral-angular intensity of radiation was investigated. In the latter case, the picture of radiation becomes more intriguing due to the interference between various physical factors such as linear and angular velocities, temperatures of the particle and vacuum background, and relative orientation of the linear and angular velocity vectors.

This work is the continuation of [16,17], where we have calculated the dissipative forces, heating and radiation of a moving spinless particle and discussed the case with particular spin orientation [18]. In this work, in contrast to [17,18], we treat the general case of relativistic translational-rotational motion of a small particle in vacuum background assuming an arbitrary mutual orientation of the linear and angular velocity vectors. Within the framework of fluctuation-electromagnetic theory, we obtain general expressions for dissipative tangential force acting on the particle, frictional torque, the rate of heating and intensities of thermal and nonthermal radiation. All particular results obtained previously stem from these expressions. The interrelation between different physical factors and their temporal dependence is discussed on an example of nanoparticles with simple form of the low-frequency polarizability. Numerical estimations correspond to graphite nanoparticles.

2. Basic assumptions and theoretical relations

We adopt quasistationary conditions assuming that a small neutral spherical particle with radius R and local temperature T_1 (in the own frame of reference Σ'') moves with linear velocity \mathbf{V} with respect to the vacuum background (reference frame Σ) and rotates with angular velocity $\mathbf{\Omega} = \Omega \mathbf{n}$ in co-moving frame Σ' (Fig. 1). The vacuum background is filled with equilibrium photonic gas with radiation temperature T_2 . During emission of the low-frequency photons, the particle is assumed to be a point-like dipole with fluctuating dipole and magnetic moments $\mathbf{d}(t), \mathbf{m}(t)$. This implies that the conditions $\Omega R/c \ll 1$, $R \ll \min(2\pi\hbar c/k_B T_1, 2\pi\hbar c/k_B T_2)$ are satisfied, where \hbar, k_B, c – are the Planck and Boltzmann constants and the speed of light in vacuum. Material properties of the particle are described by the frequency-dependent dielectric/magnetic polarizabilities $\alpha_e(\omega)$, $\alpha_m(\omega)$ which are given in the particle reference frame Σ'' . Throughout the paper we use the Gauss units.

Let the surface σ encircles the particle at a large enough distance so that the fluctuating electromagnetic field at σ can be considered as the wave field. According to the energy conservation law for the system in volume (V) restricted by σ , one may write

$$-\frac{dW}{dt} = \oint_{\sigma} \mathbf{S} \cdot d\vec{\sigma} + \int_{(V)} \langle \mathbf{j} \cdot \mathbf{E} \rangle d^3 r \quad (1)$$

where $W = (1/8\pi) \int_{(V)} (\langle \mathbf{E}^2 \rangle + \langle \mathbf{H}^2 \rangle) d^3r$ is the energy of fluctuating field in volume (V),

$\mathbf{S} = (c/4\pi) \langle \mathbf{E} \times \mathbf{H} \rangle$ is the Pointing vector, \mathbf{E} and \mathbf{H} are the corresponding electric and magnetic fields, and \mathbf{j} the density current. The angular brackets denote the total quantum and statistical averaging and all physical quantities correspond to the reference frame Σ , if not specified.

In quasistationary regime, $dW/dt = 0$, from (1) one obtains

$$I = \oint_{\sigma} \mathbf{S} \cdot d\vec{\sigma} = - \int_{(V)} \langle \mathbf{j} \cdot \mathbf{E} \rangle d^3r \equiv I_1 - I_2 \quad (2)$$

where $I_1 = I_1(T_1)$ is the intensity of radiation in vacuum, and $I_2 = I_2(T_2)$ –the intensity of radiation coming from vacuum and absorbed by the particle.

Using relativistic transformations of the density current and charge, the electric field and volume in frames Σ and Σ' , one obtains ($\beta = V/c$) [3]

$$\int_{V'} \langle \mathbf{j}' \cdot \mathbf{E}' \rangle d^3r' = \frac{1}{1-\beta^2} \left(\int_V \langle \mathbf{j} \cdot \mathbf{E} \rangle d^3r - F_x \cdot V \right) \equiv \frac{1}{1-\beta^2} dQ/dt, \quad (3)$$

$$dQ/dt = \langle \mathbf{d} \cdot \mathbf{E} + \mathbf{m} \cdot \mathbf{H} \rangle, \quad (4)$$

$$F_x = \int \langle \rho E_x \rangle d^3r + \frac{1}{c} \int \langle \mathbf{j} \times \mathbf{H} \rangle_x d^3r = \langle \nabla_x (\mathbf{d} \cdot \mathbf{E} + \mathbf{m} \cdot \mathbf{H}) \rangle. \quad (5)$$

Up to this point formulas (1)-(5) coincide with those in [20], where the particle has no own rotation. However, all physical values depend implicitly on the angular velocity $\mathbf{\Omega}$, while the particle experiences the action of frictional torque M_n

$$M_n = \langle (\mathbf{d} \times \mathbf{E} + \mathbf{m} \times \mathbf{H}) \mathbf{n} \rangle. \quad (6)$$

The work of the fluctuating field in Σ' (Eq. (3)) is spent on stopping particle rotation and its heating,

$$\int_{(V')} \langle \mathbf{j}' \cdot \mathbf{E}' \rangle d^3r' = \langle \mathbf{d}' \cdot \mathbf{E}' \rangle = \dot{Q}'' + M'_x \Omega \cos \theta + M'_y \Omega \sin \theta, \quad (7)$$

where $\dot{Q}'' = dQ''/dt'' = C_0 dT_1/dt''$ is the particle heating rate in its rest frame Σ'' (C_0 is the particle heat capacity). With allowance for the latter relationship, Eqs. (3), (7) and relativistic

transformations of torque $M'_x = \gamma M_x$, $M'_y = M_y$ and time $dt'' = dt' = \gamma^{-1} dt$ ($\gamma = (1 - \beta^2)^{-1/2}$ is the Lorentz-factor) one obtains

$$C_0 dT_1 / dt = \gamma dQ / dt - \frac{M_n \Omega}{\gamma \sqrt{1 - \beta^2 \cos^2 \theta}}. \quad (8)$$

Eq. (8) allows one to trace the evolution of the own particle temperature according to the time in resting system Σ .

Eqs. (4)–(6) are the basis for further analysis. The calculations in the right-hand sides of (4)–(6) are performed using our method [9], by representing the dipole moments and fields as the sums of spontaneous and induced components and calculating their pair correlation products with the use of fluctuation-dissipation relations. In contrast to [20, 21], the needed fluctuation-dissipation relations of the dipole moments in Σ'' are modified by the particle rotation. The elements of transformation matrix linking the vector components in Σ' and Σ'' are given by

$$A_{ik} = n_i n_k + (\delta_{ik} - n_i n_k) \cos \Omega t' - e_{ikl} n_l \sin \Omega t', \quad (9)$$

where $n_i = (\cos \theta, \sin \theta, 0)$ are the components of the unit vector \mathbf{n} in direction $\mathbf{\Omega}$ (Fig. 1). By the condition $R\Omega/c \ll 1$ we have the same time $t' = t''$ in Σ' and Σ'' .

Using (9), the fluctuation-dissipation relations for spontaneous and induced dipole moments in co-moving frame of reference Σ' take the form

$$\left\langle d^{sp'}_x(\omega') d^{sp'}_x(\omega) \right\rangle = \frac{1}{2} 2\pi \hbar \delta(\omega + \omega') \cdot \left\{ 2 \cos^2 \theta \alpha_e''(\omega) \coth \frac{\hbar \omega}{2k_B T_1} + \sin^2 \theta \left[\alpha_e''(\omega^+) \coth \frac{\hbar \omega^+}{2k_B T_1} + \alpha_e''(\omega^-) \coth \frac{\hbar \omega^-}{2k_B T_1} \right] \right\}, \quad (10)$$

$$\left\langle d^{sp'}_y(\omega') d^{sp'}_y(\omega) \right\rangle = \frac{1}{2} 2\pi \hbar \delta(\omega + \omega') \cdot \left\{ 2 \sin^2 \theta \alpha_e''(\omega) \coth \frac{\hbar \omega}{2k_B T_1} + \cos^2 \theta \left[\alpha_e''(\omega^+) \coth \frac{\hbar \omega^+}{2k_B T_1} + \alpha_e''(\omega^-) \coth \frac{\hbar \omega^-}{2k_B T_1} \right] \right\}, \quad (11)$$

$$\left\langle d^{sp'}_z(\omega') d^{sp'}_z(\omega) \right\rangle = \frac{1}{2} 2\pi \hbar \delta(\omega + \omega') \cdot \left[\alpha_e''(\omega^+) \coth \frac{\hbar \omega^+}{2k_B T_1} + \alpha_e''(\omega^-) \coth \frac{\hbar \omega^-}{2k_B T_1} \right], \quad (12)$$

$$\begin{aligned}
\left\langle d^{sp_x'}(\omega')d^{sp_z'}(\omega) \right\rangle &= -\left\langle d^{sp_z'}(\omega')d^{sp_x'}(\omega) \right\rangle = \\
&= \frac{i}{2} \sin \theta \cdot 2\pi \hbar \delta(\omega + \omega') \left[\alpha_e''(\omega^+) \coth \frac{\hbar \omega^+}{2k_B T_1} - \alpha_e''(\omega^-) \coth \frac{\hbar \omega^-}{2k_B T_1} \right],
\end{aligned} \tag{13}$$

$$\begin{aligned}
\left\langle d^{sp_y'}(\omega')d^{sp_z'}(\omega) \right\rangle &= -\left\langle d^{sp_z'}(\omega')d^{sp_y'}(\omega) \right\rangle = \\
&= -\frac{i}{2} \cos \theta \cdot 2\pi \hbar \delta(\omega + \omega') \left[\alpha_e''(\omega^+) \coth \frac{\hbar \omega^+}{2k_B T_1} - \alpha_e''(\omega^-) \coth \frac{\hbar \omega^-}{2k_B T_1} \right],
\end{aligned} \tag{14}$$

where $\omega_{\pm} = \omega \pm \Omega$, α_e'' is the imaginary component of the electric polarizability. The same expressions are valid for the magnetic dipole moments when replacing $\alpha_e \rightarrow \alpha_m$.

3. Frictional force, heating rate and frictional torque

Using (4)–(6) and (10)–(14), the calculations are performed in line with [20, 21]. The resultant expressions have the form

$$\begin{aligned}
F_x &= -\frac{\hbar \gamma}{4\pi c^4} \int_{-\infty}^{+\infty} d\omega \omega^4 \int_{-1}^1 dx x \cdot \\
&\left\{ \begin{aligned} &\left[(1 - \beta^2)(1 - x^2) \cos^2 \theta + ((1 + \beta^2)(1 + x^2) + 4\beta x) \frac{\sin^2 \theta}{2} \right] \cdot \\ &\alpha''(\omega_{\beta}) \left(\coth \frac{\hbar \omega}{2k_B T_2} - \coth \frac{\hbar \omega_{\beta}}{2k_B T_1} \right) + \\ &+ \left[(1 - \beta^2)(1 - x^2) \sin^2 \theta + ((1 + \beta^2)(1 + x^2) + 4\beta x) \frac{1 + \cos^2 \theta}{2} \right] \cdot \\ &\alpha''(\omega_{\beta} + \Omega) \left(\coth \frac{\hbar \omega}{2k_B T_2} - \coth \frac{\hbar(\omega_{\beta} + \Omega)}{2k_B T_1} \right) \end{aligned} \right\} \tag{15}
\end{aligned}$$

$$\begin{aligned}
\dot{Q} &= \frac{\hbar \gamma}{4\pi c^3} \int_{-\infty}^{+\infty} d\omega \omega^4 \int_{-1}^1 dx (1 + \beta x) \cdot \\
&\left\{ \begin{aligned} &\left[(1 - \beta^2)(1 - x^2) \cos^2 \theta + ((1 + \beta^2)(1 + x^2) + 4\beta x) \frac{\sin^2 \theta}{2} \right] \cdot \\ &\cdot \alpha''(\omega_{\beta}) \left(\coth \frac{\hbar \omega}{2k_B T_2} - \coth \frac{\hbar \omega_{\beta}}{2k_B T_1} \right) + \\ &+ \left[(1 - \beta^2)(1 - x^2) \sin^2 \theta + ((1 + \beta^2)(1 + x^2) + 4\beta x) \frac{1 + \cos^2 \theta}{2} \right] \cdot \\ &\cdot \alpha''(\omega_{\beta} + \Omega) \left(\coth \frac{\hbar \omega}{2k_B T_2} - \coth \frac{\hbar(\omega_{\beta} + \Omega)}{2k_B T_1} \right) \end{aligned} \right\}, \tag{16}
\end{aligned}$$

$$M_n = -\frac{\hbar \gamma}{4\pi c^3} \int_{-\infty}^{+\infty} d\omega \omega^3 \int_{-1}^1 dx \alpha''(\omega_\beta + \Omega) \cdot \left[\left((1+x^2)(1+\beta^2) + 4\beta x \right) \cos^2 \theta + (3-x^2 + 2\beta x) \frac{\sin^2 \theta}{2\gamma} \right] \left(\coth \frac{\hbar \omega}{2k_B T_2} - \coth \frac{\hbar(\omega_\beta + \Omega)}{2k_B T_1} \right), \quad (17)$$

where $\omega_\beta = \gamma\omega(1 + \beta x)$, $\alpha'' = \alpha''_e + \alpha''_m$. Eqs. (15)–(17) coincide with previously obtained results [20, 21] and [14].

4. Intensity of radiation

Using (2) and (3), the intensity of radiation is given by

$$I = I_1 - I_2 = -\left(\frac{dQ}{dt} + F_x V \right). \quad (18)$$

Substituting (15) and (16) in (18) yields

$$I = I_1(T_1) - I_2(T_2) = \frac{\hbar \gamma}{4\pi c^3} \int_{-\infty}^{+\infty} d\omega \omega^4 \int_{-1}^1 dx \cdot \left\{ \begin{aligned} & \left[(1-\beta^2)(1-x^2) \cos^2 \theta + \left((1+\beta^2)(1+x^2) + 4\beta x \right) \frac{\sin^2 \theta}{2} \right] \cdot \\ & \alpha''(\omega_\beta) \left(\coth \frac{\hbar \omega_\beta}{2k_B T_1} - \coth \frac{\hbar \omega}{2k_B T_2} \right) + \\ & + \left[(1-\beta^2)(1-x^2) \sin^2 \theta + \left((1+\beta^2)(1+x^2) + 4\beta x \right) \frac{1+\cos^2 \theta}{2} \right] \cdot \\ & \alpha''(\omega_\beta + \Omega) \left(\coth \frac{\hbar(\omega_\beta + \Omega)}{2k_B T_1} - \coth \frac{\hbar \omega}{2k_B T_2} \right) \end{aligned} \right\}. \quad (19)$$

Using (19), it is not difficult to obtain the corresponding spectral-angular distributions of radiation. Eqs. (16)–(19) are the main results of this work.

5. Nonthermal radiation, frictional force and torque, heating rate

A very important consequence of (15) and (19) at $\Omega \neq 0$ is the existence of nonthermal radiation in the system “particle-vacuum” and effective viscosity of vacuum caused by this radiation. By performing the limiting transition $T_1 \rightarrow 0, T_2 \rightarrow 0$ in (19) and (15) one obtains

$$\begin{aligned}
I^{(0)} &\equiv I_1(0) = \frac{\hbar \gamma}{2\pi c^3} \int_{-1}^1 dx \cdot f(x, \theta) \int_0^{\Omega \gamma^{-1}(1+\beta x)^{-1}} d\omega \omega^4 \alpha''(\Omega - \gamma \omega(1 + \beta x)) = \\
&= \frac{4\hbar}{3\pi c^3} \int_0^{\Omega} d\xi \xi^4 [\alpha_e''(\Omega - \xi) + \alpha_m''(\Omega - \xi)],
\end{aligned} \tag{20}$$

$$f(x, \theta) = (1 - \beta^2)(1 - x^2) \sin^2 \theta + \left((1 + \beta^2)(1 + x^2) + 4\beta x \right) \frac{1 + \cos^2 \theta}{2}, \tag{21}$$

$$F_x^{(0)} = -\frac{4\hbar V}{3\pi c^5} \int_0^{\Omega} d\xi \xi^4 [\alpha_e''(\Omega - \xi) + \alpha_m''(\Omega - \xi)] \tag{22}$$

The last line of Eq. (20) agrees with [3] and [17] in the case of rotating body without translational motion. As one can see from the right-hand side of Eq. (20), the integrated emission intensity of the system “particle-vacuum” is the direct result of particle rotation, and it does not depend on the magnitude and direction of linear velocity. From (22) it follows that a particle in translational-rotational motion experiences the action of a drag force in cold vacuum. The friction coefficient is independent on the magnitude and direction of the linear velocity, and vanishes at $\Omega = 0$. From (20) and (22) it follows

$$F_x = -\frac{\beta}{c} \cdot I^{(0)}. \tag{23}$$

Therefore, the drag force is caused by the nonthermal radiation, and the photons are emitted predominantly in the forward direction.

Other important aspects of cold conditions concern the frictional torque and the particle heating. Performing the transitions $T_1 \rightarrow 0, T_2 \rightarrow 0$ in (17) and integrating over x yields

$$M_n = -\frac{4\hbar}{3\pi c^3 \gamma} (\cos^2 \theta + \gamma \sin^2 \theta) \cdot \int_0^{\Omega} d\xi \xi^3 [\alpha_e''(\Omega - \xi) + \alpha_m''(\Omega - \xi)] \tag{24}$$

From (24) it follows that $M_n < 0$ at any form of the functions $\alpha_{e,m}''(\omega)$, i. e. the torque decelerates the particle rotation.

With allowance for (18), (20), (22) and (24), Eq. (8) reduces to

$$\begin{aligned}
C_0 \frac{dT_1}{dt} &= \frac{4\hbar \Omega}{3\pi c^3 \gamma^2} \frac{(\cos^2 \theta + \gamma \sin^2 \theta)}{\sqrt{1 - \beta^2 \cos^2 \theta}} \cdot \int_0^{\Omega} d\xi \xi^3 [\alpha_e''(\Omega - \xi) + \alpha_m''(\Omega - \xi)] - \\
&- \frac{4\hbar}{3\pi c^3 \gamma} \int_0^{\Omega} d\xi \xi^4 [\alpha_e''(\Omega - \xi) + \alpha_m''(\Omega - \xi)]
\end{aligned} \tag{25}$$

Eq. (25) shows that the particle temperature increases with time, since the second term is the right-hand side of Eq. (25) is usually dominating (except strongly exotic conditions

$\gamma \gg 1, \theta = 0$). Notwithstanding the fact that condition $T_1 \equiv 0$ is not preserved all the time, the temperature T_1 can be very close to zero for a long time, depending mainly on the particular values of Ω and material properties. For example, using (25) and assuming $\gamma = 1, C_0 \sim T$ (at low temperature for metals) and $\alpha''(\omega) \sim \omega$ (typical low-frequency dependence of polarizability), the time τ of increasing the particle temperature from zero to T_1 scales as $\tau \propto T_1^2 / \Omega^6$ (i. e. $\tau \rightarrow \infty$ at $\Omega \rightarrow 0$). In this case, $|F_x| \propto V \Omega^6, I^{(0)} \propto \Omega^6$, and $|M_n| \propto \Omega^5$, while the characteristic times of angular and linear deceleration turn out to be much longer than τ [21, 22]. More details relating the temporal dependences of T_1, Ω, V and their interrelation are discussed in Sect. 4.

6. Finite temperatures and temporal dependences of T_1, Ω and V

In order to simplify the analysis of general results, we adopt a simple form of the dielectric polarizability of spherical nonmagnetic particle: $\alpha''(\omega) = 3R^3\omega/4\pi\sigma_0$, where σ_0 is the static conductivity. This corresponds to the law-frequency limit of the Drude-like dielectric permittivity $\varepsilon(\omega) = i \cdot 4\pi\sigma_0/\omega$. In this case, using (15), (19) and (17) and denoting $\mathcal{G}_{1,2} = k_B T_{1,2} / \hbar$, the integrals are calculated explicitly and one obtains

$$F_x = -\frac{8\pi^4}{21} \frac{\hbar R^3}{c^4 \sigma_0} \beta \left[\frac{(1 + \beta^2/5)}{(1 - \beta^2)} \mathcal{G}_2^6 + \mathcal{G}_1^6 \psi_1(\Omega/\mathcal{G}_1) \right], \quad (26)$$

$$I \equiv I_1 - I_2 = \frac{8\pi^4}{21} \frac{\hbar R^3}{c^3 \sigma_0} \left[\mathcal{G}_1^6 \psi_1(\Omega/\mathcal{G}_1) - \frac{(1 + \beta^2)}{(1 - \beta^2)} \mathcal{G}_2^6 \right], \quad (27)$$

$$M_n = -\frac{2\pi^2}{15} \frac{\hbar R^3 \Omega}{c^3 \sigma_0} \left[(\gamma(1 + \beta^2) \cos^2 \theta + \sin^2 \theta) \mathcal{G}_2^4 + \left(\frac{\cos^2 \theta}{\gamma} + \sin^2 \theta \right) \psi_2(\Omega/\mathcal{G}_1) \mathcal{G}_1^4 \right], \quad (28)$$

$$\psi_1(x) = 1 + \frac{21}{10\pi^2} x^2 + \frac{7}{8\pi^4} x^4 + \frac{7}{80\pi^6} x^6, \quad (29)$$

$$\psi_2(x) = 3 + \frac{5}{2\pi^2} x^2 + \frac{3}{8\pi^4} x^4, \quad (30)$$

Combining Eqs. (8), (18), (26)–(28) yields

$$C_0 dT_1 / dt = \frac{8\pi^4}{21} \frac{\hbar R^3}{c^3 \sigma_0} \left[\frac{(1 + 2\beta^2 + \beta^4/5)}{(1 - \beta^2)^{3/2}} \mathcal{G}_2^6 - (1 - \beta^2)^{1/2} \psi_1(\Omega/\mathcal{G}_1) \mathcal{G}_1^6 \right] - \frac{M_n \Omega}{\gamma \sqrt{1 - \beta^2 \cos^2 \theta}} \quad (31)$$

An important consequence of (26) and (27) is their independence on the angle θ . The torque M_n depends on θ , being always negative. As follows from the structure of (26)–(28) and (31), the contribution of angular velocity Ω becomes important only when $\Omega/\mathcal{G}_1 > 1$, increasing the rate of particle heating (through the contribution of M_n in (31)), frictional force and intensity of radiation (the terms proportional to \mathcal{G}_1^6 in (26), (27)). As long as $\Omega/\mathcal{G}_{1,2} \gg 1$, the contribution of particle rotation to F_x, I, M_n and dT_1/dt is described by (22), (20), (24) and (25).

In order to compare the characteristic times of particle heating, linear and rotational deceleration, we should also invoke the dynamics equations

$$mcd\beta/dt = (1 - \beta^2)^{3/2} F_x \quad (32)$$

$$Id\Omega/dt = \frac{M_n}{\gamma \sqrt{1 - \beta^2 \cos^2 \theta}}, \quad (33)$$

where $I = 2mR^2/5$ is the inertia moment in the reference frame of particle, and m the particle mass. Using (31)–(33) with allowance for (26), (28), (31), equations (31)–(33) take dimensionless form (Eqs. (A1)–(A3) in Appendix) when introducing the time scales τ_Q, τ_β and τ_Ω , corresponding to the thermal relaxation, linear and angular deceleration, respectively

$$\tau_Q = \frac{7}{2\pi^3} \frac{c^3 \sigma_0 C_s \rho}{k_B \mathcal{G}_2^5}, \quad (34)$$

$$\tau_\beta = \frac{7}{2\pi^3} \frac{c^5 \sigma_0 \rho}{\hbar \mathcal{G}_2^6}, \quad (35)$$

$$\tau_\Omega = \frac{4}{\pi} \frac{c^3 \sigma_0 \rho R^2}{\hbar \mathcal{G}_2^4}. \quad (36)$$

Simple analysis of (34)–(36) shows that $\tau_Q \ll \tau_\Omega \ll \tau_\beta$ for conducting nanoparticles in a wide range of temperatures. For example, for graphite particles at $T_2 = 300 K$, $\sigma_0 = 2 \cdot 10^{14} s^{-1}$, $C_s = 7 \cdot 10^6 erg/g \cdot K$, $\rho = 2.1 g/cm^3$, $R = 10 nm$ we obtain $\tau_Q = 0.7 s$, $\tau_\Omega = 5.7 \cdot 10^6 s$, and $\tau_\beta = 2.9 \cdot 10^{11} s$. Therefore, when calculating stopping times of translational and rotational motion from (A1), (A3), one may fix the ratio T_1/T_2 , and parameters Ω, β . On the other hand,

when calculating the time of thermal relaxation from (A2), one may fix the values of Ω and β . More accurate numerical calculations of thermal and dynamical relaxation using (A1)–(A3) do not violate the interrelation between the characteristic times involved as compared to the inequality $\tau_Q \ll \tau_\Omega \ll \tau_\beta$ [20, 21].

Therefore, the leading parameter in the particle dynamics is its temperature T_1 . The intensity of radiation (at fixed T_2) is also determined by T_1 , while the dependence on the linear and angular velocity affects in an indirect way through T_1 . Irrespectively of the initial ratio between T_1 and T_2 , temperature T_1 quickly tends to the quasistationary value, so does the intensity of radiation.

Two important cases are worth noting when $T_1 \neq T_2$ (with T_1 being the initial particle temperature and $T_2 = \text{const}$): i) $t < \tau_s$; ii) $t > \tau_s$, where τ_s is the thermal relaxation time which is proportional to τ_Q .

At $t < \tau_s$ and $T_1 < T_2$ (except the case $\Omega > \mathcal{G}_2$, when $\Omega > 10^{11} \text{ s}^{-1}$ even at $T_2 = 1 \text{ K}$), the particle absorbs much more radiation (I_2) than emits (compare the second and first terms in (27)). To an outside observer, for example, a cloud of cold dust particles being injected into the area with high radiation temperature will effectively absorb thermal photons, and the absorbed power scales as γ^2 . The intensity radiated (the first term in (27)) in this case depends on the ratio between Ω and \mathcal{G}_1 . The function $\mathcal{G}_1^6 \psi_1(\Omega/\mathcal{G}_1)$ reaches a maximum value at $\Omega/\mathcal{G}_1 = 4.78$, and the maximum of I_1 is an order of magnitude higher than intensity $I^{(0)}$ of nonthermal radiation (Eq. (20)). At $t < \tau_s$ and $T_1 > T_2$ the initial ratio I_1/I_2 strongly depends on β and can be both < 1 (at $\gamma \gg 1$) and > 1 (at $\gamma \rightarrow 1$).

At $t > \tau_s$, the temperature reaches the quasistationary value which is determined by equating the right-hand side of (31) to zero. In this case the ratio I_1/I_2 between emitted and absorbed radiation intensities exceeds the unit. It scales as γ^2 and increases with Ω/\mathcal{G}_2 . The case when the particle temperature reaches the melting point needs a special analysis (see also [20]).

The temporal dependences of T_1/T_2 and I_1/I_2 for graphite particles are illustrated by Figs. 1, 2, assuming $T_2 = \text{const}$. On both figures, the solid and dashed lines correspond to $\beta = 0.1$ and $\beta = 0.999$. Thin lines (solid and dashed) correspond to the initial ratio $T_1/T_2 = 3$, while thick lines (solid and dashed) correspond to the initial ratio $T_1/T_2 = 0.01$. The time scale in Fig. 3 is given in units τ_Q , while the time scale in Fig. 4 is given in units τ_s (individual for each curve).

In all the cases we assumed that $\Omega/\mathcal{G}_1 = 1$ and $\theta = \pi/2$, since the variation of these parameters insignificantly changes the general picture (until $\Omega/\mathcal{G}_1 < 10$). One can see that T_1 and I_1 quickly tend to the quasistationary values. Further on, at $t \gg \tau_s$ parameters β and Ω monotonously decrease with time, $T_1 \rightarrow T_2$ and $I_1 \rightarrow I_2$ until the particle is stopped.

7. Conclusions

We have obtained a full set of equations describing the fluctuation-electromagnetic interaction, dynamics and kinetics of heating of a small polarizable particle with arbitrary direction of spin moving in the vacuum background at arbitrary temperatures of particle and background. The obtained equations allows to calculate the thermal and dynamical state of the particle in dependence of time.

At zero temperature of particle and radiation background, the particle emits the long-wavelength photons. The corresponding intensity depends on the angular velocity and does not depend on the linear velocity and the spin direction. Despite the particle is heated, the state $T_1 \approx 0$ can be preserved for a rather long time.

We have analyzed the case of finite temperatures of the particle and background assuming that the particle polarizability is proportional to frequency. As in the “cold” case, the tangential force and radiation intensity do not depend on the spin orientation (though depend on the angular velocity). We have shown that the temporal dependence of the full set of dynamic parameters for conducting particles is determined by the particle temperature (in the rest frame of particle), since the time of thermal relaxation is much less than the times of stopping (rotation and uniform motion). The particle temperature relaxes to the quasistationary value depending on the temperature of radiation background, the linear velocity and the state of rotation (to less extent). The maximum intensity of radiation in the quasistationary state is proportional to γ^2 . Further on, the difference between the emitted and absorbed intensity of radiation fades with time until the particle is stopped. The initially cold particle predominantly absorbs the vacuum radiation in the phase of heating and the rate of absorption also scales as γ^2 . We believe that along with their fundamental importance, our results will be important for trapping nanoparticles in cavities and in astrophysics of dust matter.

References

- [1] H.B.G. Casimir, Proc. K. Ned. Akad. Wet. 51 (1948) 793.
- [2] D.A.R. Dalvit, P.A. Maia Neto, and F. D. Mazzitelli, Lecture Notes in Physics. 834 (2011) 419.
- [3] Ya. B. Zel'dovich, JETP. Lett.. 14 (1971)180.
- [4] M.S. Tomassone, A. Widom, Phys. Rev. B56 (1997) 4938.
- [5] G.V. Dedkov G V and A.A. Kyasov, Phys. Solid State 44/10(2002) 1809.
- [6] V.A. Mkrtchian, V.A. Parsegian, R. Podgornik and W.M. Saslow, Phys. Rev. Lett. 91 (2003) 220801.
- [7] J.R. Zurita-Sanchez, J.J. Greffet, and L. Novotny, Phys. Rev. A69 (2004) 022902.
- [8] F. Intravaia, C. Henkel, and M. Antezza, Lecture Notes in Physics. 834 (2011) 345.
- [9] G.V. Dedkov and A.A. Kyasov , J. Phys.: Condens. Matter 20 (2008) 354006.
- [10] S.Y. Buchmann and D. Welsch, Phys. Rev. A77 (2008) 012110.
- [11] G. Barton, New J. Phys. 12(2010) 113045.
- [12] J.S. Høye and I. Brevik 2011 Eur. Phys. J. D64 (2011) 1.
- [13] J.S. Høye and I. Brevik , Eur. Phys. J. D68 (2014)161.
- [14] A. Manjavacas and F. J. Garcia de Abajo, Phys. Rev. A82 (2010) 063827(1–10).
- [15] R. Zhao, A. Manjavacas, F.G. Garcia de Abajo, and J.B. Pendry, Phys. Rev. Lett. 109 (2012) 2123604.
- [16] G.V. Dedkov, A.A. Kyasov, Eur. Phys. Lett. 99 (2012) 64002
- [17] M.F. Maghrebi, R.L. Jaffe, and M. Kardar, Phys. Rev. Lett. 108 (2012) 230403 (1–14).
- [20] G.V. Dedkov, AA. Kyasov, Phys. Scripta, 89 (2014) 105501(1–7)
- [21] A.A. Kyasov, G.V. Dedkov, Arm. J. Phys. 7/ 4. (2014)177.

Appendix

$$d\beta/d\tau = -\beta(1-\beta^2)^{3/2} \left[\frac{1+\beta^2/5}{(1-\beta^2)} + x^6 \psi_1(y/x) \right] \quad (\text{A1})$$

$$dx/d\tau = \left[\frac{1+2\beta^2+\beta^4/5}{(1-\beta^2)^{3/2}} - (1-\beta^2)^{1/2} x^6 \psi_1(y/x) \right] + \frac{7}{20\pi^2} \frac{y^2}{\gamma(1-\beta^2 \cos^2 \theta)^{1/2}} \cdot \left[\gamma(1+\beta^2) \cos^2 \theta + \sin^2 \theta + \left(\frac{\cos^2 \theta}{\gamma} + \sin^2 \theta \right) \psi_2(y/x) x^4 \right] \quad (\text{A2})$$

$$dy/d\tau = -\frac{y}{\gamma(1-\beta^2 \cos^2 \theta)^{1/2}} \left[\gamma(1+\beta^2) \cos^2 \theta + \sin^2 \theta + \left(\frac{\cos^2 \theta}{\gamma} + \sin^2 \theta \right) \psi_2(y/x) x^4 \right] \quad (\text{A3})$$

Here $x \equiv T_1/T_2$, $y \equiv \Omega/\mathcal{G}_2$, and dimensionless time τ in (A1)–(A3) corresponds to t/τ_β , t/τ_Q , and t/τ_Ω , respectively.

FIGURE 1

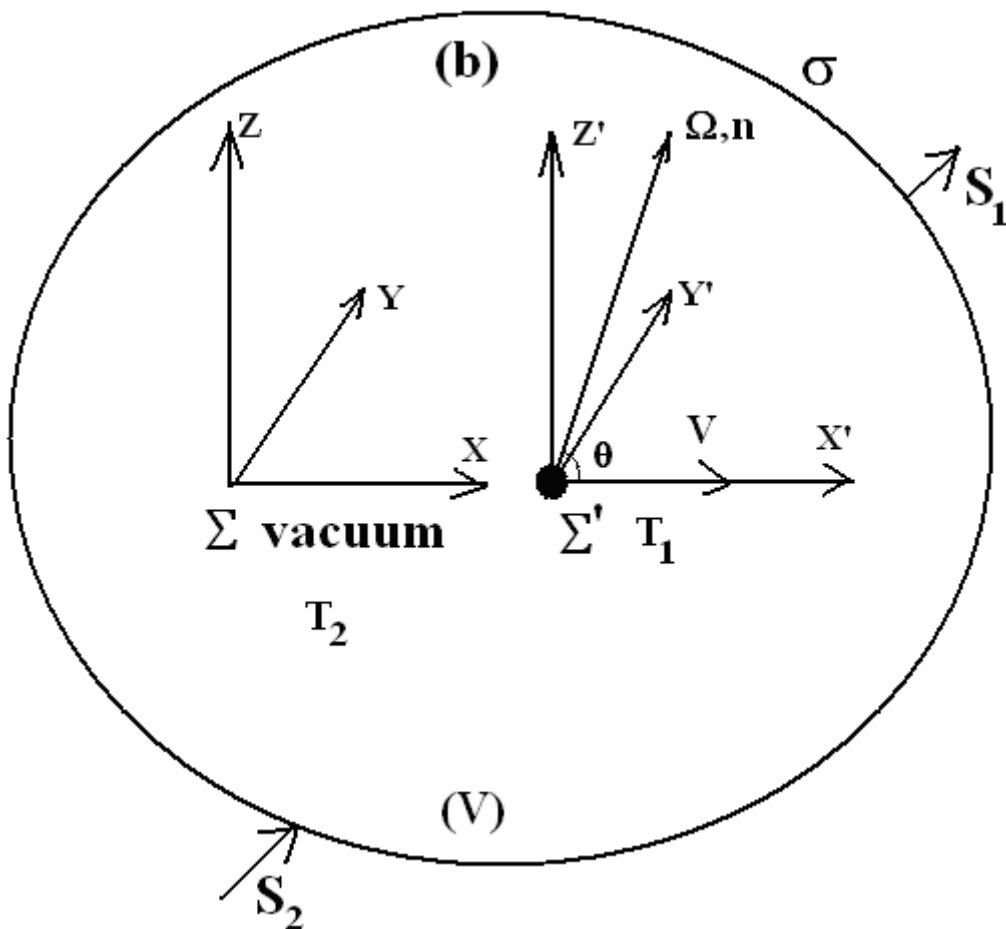


FIGURE 2

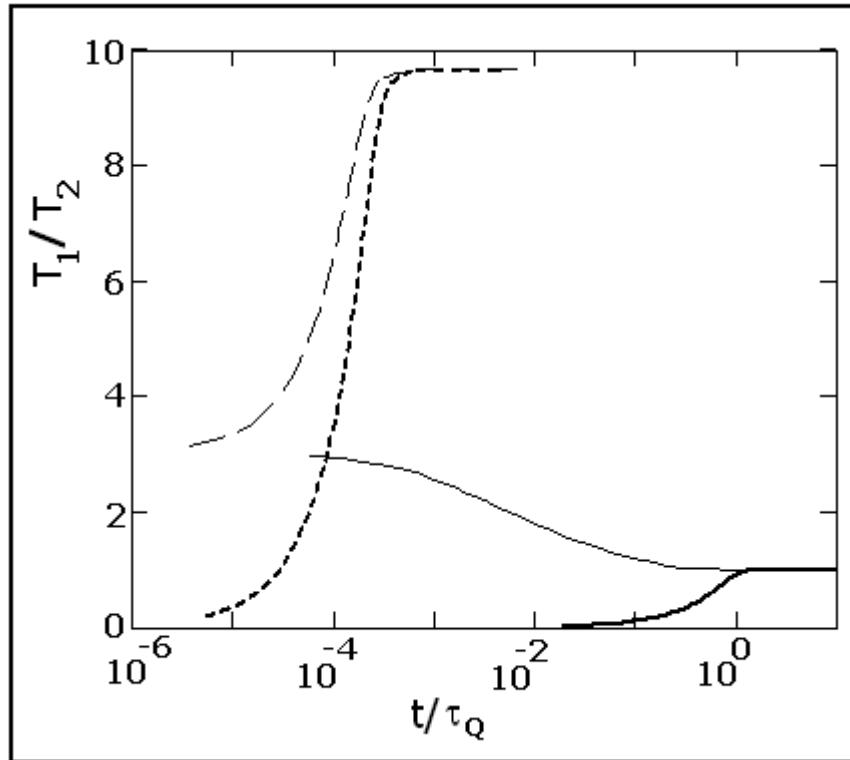


FIGURE 3

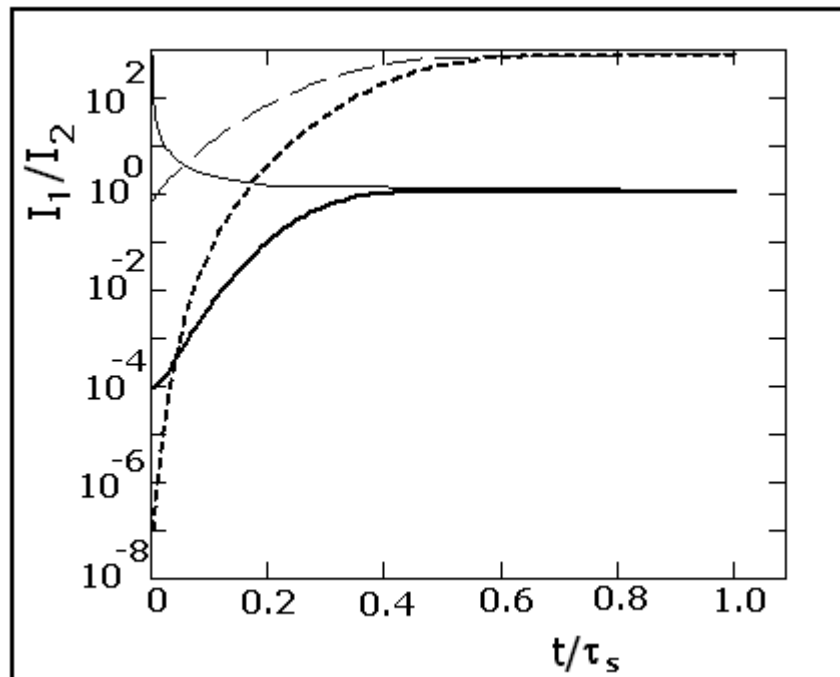


FIGURE CAPTIONS

Fig. 1

Scheme of the particle motion and coordinate systems used. The own (rest frame) system Σ'' of the particle is not shown. Its Z'' axis is directed along the vector \mathbf{n} .

Fig. 2

Temporal dependence of the T_1/T_2 according to Eq. (A2). In all cases $T_2 = \text{const}$, $\Omega/\mathcal{G}_2 = 1$, $\theta = \pi/2$, τ_Q is determined by (34). Thin solid line: $\beta = 0.1, T_1(0)/T_2 = 3$; thin dashed line: $\beta = 0.999, T_1(0)/T_2 = 3$; thick solid line: $\beta = 0.1, T_1(0)/T_2 = 0.01$; thick dashed line: $\beta = 0.999, T_1(0)/T_2 = 0.01$. $T_1(0)$ corresponds to the moment $t = 0$.

Fig. 3

Temporal dependence of the I_1/I_2 according to (27) with allowance for the temporal dependences of T_1/T_2 in Fig. 2. The correspondence of thick and solid lines is the same as in Fig. 2. The τ_s corresponds to the moment of reaching thermal equilibrium (saturation points on the curves shown in Fig. 2).